

| | |
|-------------|---|
| Title | Discussion on the mechanism of ground improvement method at the excavation of shallow overburden tunnel in difficult ground |
| Author(s) | Kishida, Kiyoshi; Cui, Ying; Nonomura, Masaichi; Iura, Tomomi; Kimura, Makoto |
| Citation | Underground Space (2016), 1(2): 94-107 |
| Issue Date | 2016-12 |
| URL | http://hdl.handle.net/2433/220413 |
| Right | © 2016 Tongji University and Tongji University Press. Production and hosting by Elsevier B.V. on behalf of Owner. This is an open access article under the CC BY-NC-ND license (http://creativecommons.org/licenses/by-nc-nd/4.0/). |
| Type | Journal Article |
| Textversion | publisher |



Discussion on the mechanism of ground improvement method at the excavation of shallow overburden tunnel in difficult ground

Kiyoshi Kishida ^{a,*}, Ying Cui ^b, Masaichi Nonomura ^c, Tomomi Iura ^d, Makoto Kimura ^e

^a Department of Urban Management, Kyoto University, Kyoto 615-8540, Japan

^b Department of Civil Engineering, Meijo University, Nagoya 468-5802, Japan

^c Railway Engineering Co. Ltd., Tokyo 105-0012, Japan

^d Japan Railway Construction, Transport and Technology Agency, Yokohama 231-8351, Japan

^e Department of Civil and Earth Resources Engineering, Kyoto University, Kyoto 615-8540, Japan

Received 30 October 2016; received in revised form 21 November 2016; accepted 22 November 2016

Available online 23 December 2016

Abstract

Tunnel construction opportunities involving shallow overburdens under difficult (e.g., soft, unconsolidated) grounds have been increasing in Japan. Various auxiliary methods for excavating mountain tunnels have been developed and can satisfy stringent construction requirements. The ground improvement method, which is one of the auxiliary methods for shallow overburden tunnels, has demonstrated its ability to effectively control the amount of settlement under soft ground. However, the mechanism of the ground improvement method has not been clarified, nor has a suitable design code been established for it. Therefore, because the strength of the improved ground and the suitable length and width of the improved area have not been fully understood, an empirical design has been applied in every case. In this paper, the mechanical behavior during the excavation, including that of the stabilized ground, is evaluated through trapdoor experiments and numerical analyses. In addition, the enhancement of tunnel stability resulting from the application of the ground improvement method is discussed.

© 2016 Tongji University and Tongji University Press. Production and hosting by Elsevier B.V. on behalf of Owner. This is an open access article under the CC BY-NC-ND license (<http://creativecommons.org/licenses/by-nc-nd/4.0/>).

Keywords: Auxiliary method; Shallow overburden; Soft ground; Ground improvement; Settlement

Introduction

When a tunnel with a shallow overburden is excavated in a difficult (e.g., soft, unconsolidated) ground, the stability and the safety of the tunnel excavating face is of concern. Particularly in the case of soft ground, the ground that is loosened by the excavation tends to expand into the surrounding ground. In addition to the shallow overburden, the excavation also has a direct effect on the ground surface above the tunnel. Therefore, control of

the loosened ground is the most important technical issue in the excavation of a tunnel located under a shallow overburden in soft ground. The cut and cover method has been widely used as the main tunneling method for excavating a shallow overburden tunnel in soft ground. Recently, use of the recently developed auxiliary method, the New Austrian Tunneling Method (NATM), has been increasing. In the construction field, when the NATM is used to excavate a shallow overburden tunnel in soft ground, an auxiliary method, such as pipe forepiling or vertical pre-reinforcement, is applied at the tunnel construction site, and stabilization of the crown and the prevention of ground surface settlement are then conducted.

Various auxiliary tunneling methods have been employed to prevent both the collapse of the tunnel excava-

* Corresponding author.

E-mail address: kishida.kiyoshi.3r@kyoto-u.ac.jp (K. Kishida).

Peer review under responsibility of Tongji University and Tongji University Press.

tion face and settlement at the surface and tunnel crown. When employing an auxiliary method, the workability and stability of the tunnel excavation should be explored, and a suitable auxiliary method should be chosen. Miwa and Ogasawara (2005) addressed the excavation of bullet train tunnels that crossed under a national highway with a shallow overburden. They reported that four excavation methods had been proposed and discussed and that NATM with the grouting-type pipe forepiling method was selected considering the safety, the construction term and the construction costs. As a result, the face was prevented from collapsing, and the tunnel was excavated while keeping ground surface settlement to a minimum and avoiding interference with road traffic. However, the effective mechanism of the grouting-type pipe forepiling method in this application was not discussed.

Several previous research works have discussed the advantages of stable tunnel excavation and the mechanisms of auxiliary methods. Since tunnels are often driven through soft ground containing groundwater and in locations close to various utilities and structures, Kimura, Ito, Iwata, and Fujimoto (2005) applied two methods, namely, special jet grouting for foot piles and long steel pipe fore-piling for preventing displacement, and a boring method for groundwater drainage. Oke, Valchopoulos, and Marinos (2014) analyzed literature and construction reports and discussed the effect of the umbrella arch (UA) by classifying three types of support elements: spiles, forepoles and grouted. Yoo (2002) investigated the behavior of a tunnel face reinforced by longitudinal pipes using a 3D finite element analysis. Based on the numerical results, he concluded that the face-reinforcement technique using longitudinal pipes could significantly reduce the deformation of the face and thus improve its stability. Kamata and Mashimo (2003) researched the effects of several auxiliary methods, such as face bolting, vertical pre-reinforcement bolting and forepiling, through centrifugal modeling tests on sandy ground and numerical simulation with DEM. They identified several favorable effects in terms of face stability. Taguchi et al. (2000) conducted model and full-size tests on a thin flexible pre-lining. They concluded that the pre-lining was effective for both the stability of the face and the prevention of ground surface settlement. They also proposed a quantitative estimation method for face stability. Kitagawa et al. (2009, 2010) performed trapdoor experiments and a numerical simulation to determine the effect of a reduction in settlement and the corresponding mechanism using a tunnel foot rein-

forcement side pile. Cui, Kishida, and Kimura (2008) performed numerical simulation of a tunnel excavation and a side pile with the aim to prevent surface settlement of the shallow overburden and the soft ground. Based on the numerical simulation, they proposed that the prevention of ground surface settlement and tunnel settlement, by the installation of a foot reinforcement side pile, affects the shear reinforcement, the load redistribution and the internal pressure. They also advised that the foot reinforcement side pile should be installed across the shear zone during tunnel excavation.

Several tunnels constructed for the Tohoku bullet train in Japan, the so-called Tohoku Shinkansen Railway, between Hachinohe and Shichinohe-Towada, were constructed under the condition of shallow overburden and soft ground. In cases without any obstacles on the ground surface, the objective ground was improved using the shallow or deep mixing stabilization method. Then, the tunnel was excavated by NATM. This approach constitutes the ground improvement method of the excavation of a shallow overburden tunnel. Fig. 1 shows the construction process associated with this method. First, the ground is excavated to the upper part of the tunnel crown. Then, cement is mixed with the natural ground around the side-wall of the tunnel using the shallow or the deep mixing stabilization method. The premixed soil is spread and compacted by rolling it over the tunnel crown area. Finally, the excavated soil is backfilled and compacted by rolling it to the ground surface. The tunnel can then be excavated using NATM. Various combinations of improved areas and levels of strength of the improved ground were implemented in the field, and the tunnels were excavated successfully. The ground improvement method was employed after considering the conditions of the overburden, the geology, the ground surface, the allowed settlement, and data from several previously reported construction projects (Kitagawa, Isogai, Okutsu, & Kawaguchi, 2004; Nonomura, Iura, Okajima, & Kishida, 2011; Saito, Ishiyama, Tano, & Haga, 2011; Tadenuma, Isogai, Konishi, Nishiyama, & Okutsu, 2003). Without disturbing any buildings and houses on the surface, this method has the advantage of pre-knowledge of the geological structure. Consequently, this method is more advantageous in terms of construction costs than other auxiliary methods, as shown in Fig. 2.

In this study, three-dimensional (3D) trapdoor experiments are conducted to simulate the progress of a tunnel excavation. In the trapdoor experiments, the

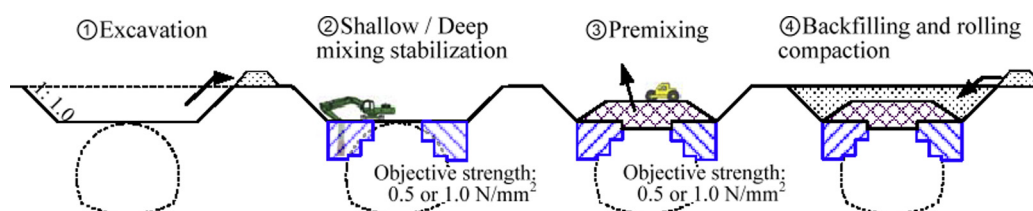


Fig. 1. Construction process of pre-ground improvement method.

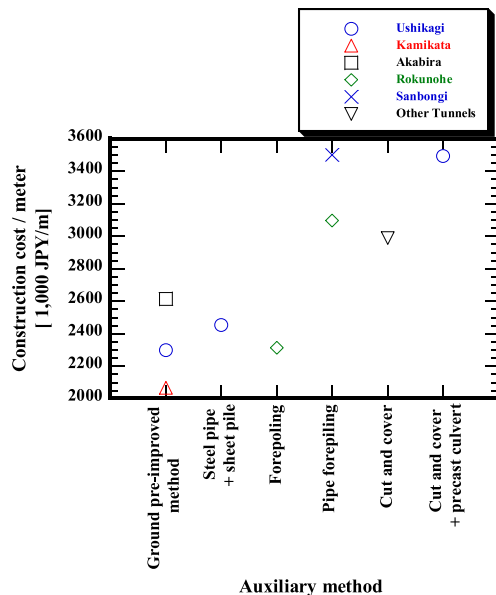


Fig. 2. Comparison of construction costs for auxiliary methods in Tohoku Shinkansen construction project between Hachinohe and Shichinohe-Towada.

tunneling process is simulated by the lowering of supporting plates (trapdoors) to reduce the confining stress in localized areas (Adachi, Kimura, & Kishida, 2003; Murayama & Matsuoka, 1971; Ono & Manai, 1938). Nakai, Xu, and Yamazaki (1997) performed 3D trapdoor model tests, using a continuous trapdoor apparatus, to investigate the 3D effect and the dilatancy effect on the ground movements occurring during tunnel excavation. Cui et al. (2008) conducted a series of model experiments using the trapdoor apparatus to clarify the effect of the foot reinforcement side pile.

In this paper, the results of trapdoor experiments are presented considering the range in improvement as a parameter. Then, the influence of this parameter on both surface settlement and earth pressure distribution points is discussed. In addition, two-dimensional (2D) elastoplastic finite element analyses, used to simulate the tunnel excavation process, are conducted to clarify the effect of the pre-ground improvement method. Based on the trapdoor experiments and the numerical simulations, the mechanism and the design concept of the ground improvement method are discussed.

Discussion on stabilizing range through 3D trapdoor experiments

3D trapdoor experiments were performed to elucidate the effect of a stabilized area. In addition, the effect on the reduction in settlement and the mechanism of the redistributed earth pressure are addressed by considering the stabilized area of the ground.

Testing apparatus and model ground

Fig. 3 shows the 3D trapdoor apparatus used in these model experiments; it was developed by Adachi et al. (2003). The soil tank is 1000 mm in both length and width. The height of the soil box can be controlled to a multiple of 75 mm. The apparatus consists of six supporting plates (①–⑥), all 150 mm in width, set along the centerline of an iron table. These plates can be moved upwards or downwards either individually or simultaneously. Load cells are installed at the bottom of each supporting plate. In this research, the tunneling excavation process is simulated by continuously lowering the supporting plates 2.0 mm, from Trapdoor 1 to Trapdoor 4. Earth pressure gauges (Gauges 1–4) are installed at the bottom of the supporting plates and the soil tank, as shown in Fig. 3b, to measure the vertical load and the earth pressure. Profiles of the ground surface are taken using a laser scan micro sensor system installed in the upper part of the soil tank. The shape of the ground surface is measured in 15 profiling lines, as shown in Fig. 3a.

The model ground is produced by dropping dried silica sand No. 6 from 600 mm above the ground surface. The relative density of the model ground is 70%. In actual construction work, an improved ground is produced with cement to increase the ground stiffness and the strength. In this experimental work, the increase in viscosity is modeled by mixing in water at a given quantity in the area of interest. The percentage of moisture weight is 5%. As the water is mixed in, suction occurs between the contact points of the sandy particles, increasing the viscosity and stiffness of the area of interest. To confirm this increase in stiffness, direct shear tests are performed to estimate the internal friction angle and cohesion under both dry and wet conditions. The internal friction angle and cohesion under a dry condition are 27.2° and 16.5 kN/m², respectively. The corresponding values under a wet condition (5% moisture weight) are 27.0° and 23.7 kN/m². It is thus confirmed that the cohesion increases with the addition of water. A guide wall is installed between the improved ground and the unimproved ground to prevent the movement of the moisture content into the unimproved ground. After the guide wall is installed, the improved ground is established; then, the guide wall is removed, and the unimproved ground is also established. To estimate the strength of the improved ground in the trapdoor experiments, a portable penetration test is performed to measure the resistance Q_c before and after the ground is improved, as shown in Table 1. The Q_c after the improvement is larger than that before the improvement at each penetration depth. The Q_c value of the improved ground was 2.2–3.3 times that of the original ground. At an actual construction site, the N value of the improved ground by the standard penetration test was 2.7–20 times of that of the original ground.

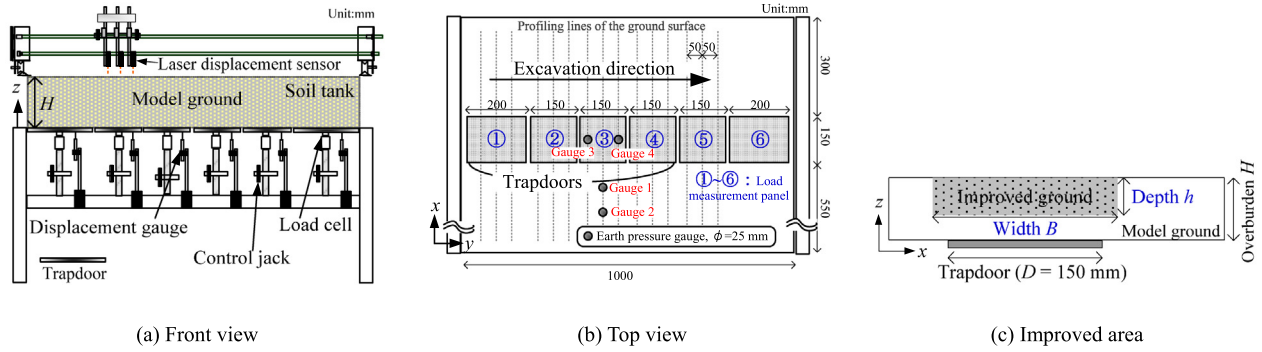


Fig. 3. Three-dimensional trapdoor apparatus, surface settlement profiling system (Adachi et al., 2003) and set-up of trapdoors, earth pressure gauges and installed improved ground.

Table 1
Penetration resistance, Q_c .

| Depth of penetration [cm] | Q_c before improvement [kN/m ²] | Q_c after improvement [kN/m ²] | Ratio |
|---------------------------|---|--|-------|
| 5.0 | 72.7 | 238.7 | 3.3 |
| 10.0 | 201.2 | 526.2 | 2.6 |
| 15.0 | 335.1 | 738.7 | 2.2 |

Table 2
Experiment cases.

| Overburden ratio, H/D | Depth of improved ground, h [mm] | Width of improved ground, B [mm] | | | |
|-------------------------|------------------------------------|------------------------------------|-----|--------|--------|
| | | 0 | 150 | 250 | 350 |
| 1.0 | 0 | Case-1 | | | |
| | 50 | | | Case-2 | |
| | 100 | Case-3 | | Case-4 | Case-5 |
| 0.5 | 0 | Case-6 | | | |
| | 50 | Case-7 | | Case-8 | |

Experiment cases

The position and an image of the improved ground are presented in Fig. 3c. Model experiments were conducted under two overburden conditions, namely, $H/D = 1.0$ and $H/D = 0.5$, where H is the height of the model ground and D is the width of the trapdoor (150 mm). The height of the soil tank under the overburden conditions of $H/D = 1.0$ and $H/D = 0.5$ was 150 and 75 mm, respectively. Model experiments were conducted for 8 cases by changing the improved width, B , the depth, h , and the ground height, H , as shown in Table 2.

Experimental results

Surface settlement at H/D of 1.0

Fig. 4 shows the surface settlement occurring on the centerline of Trapdoor 3, termed Line 8 for Case 1, without any ground improvement. The four lines show the settlement shapes of the ground surface along Line 8 when Trapdoors 1 to 4 are lowered. There is almost no change when Trapdoors 1 and 2 are lowered. However, the surface sinks by a large value when Trapdoor 3 is lowered and by an even larger value when Trapdoor 4 is lowered. If Trapdoor 3 is taken as the tunnel excavating face, i.e., Line 8 is the tunnel face, then the process of lowering Trapdoors 1 and 2 can be thought of as the displacement ahead of the face. There is almost no displacement ahead of the face occurring in the tunnel excavation process; a large part of the settlement occurs when the tunnel face arrives at Line 8.

Fig. 5a shows the shapes of the surface settlement measured on the profiling line, Line 8, when Trapdoor 3 is low-

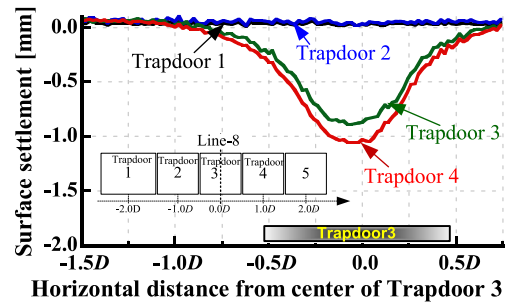


Fig. 4. Change in surface settlement along Line-8 in Case-1 (without improved ground).

ered for the cases of the improved ground with different widths and depths. The maximum surface settlements occur in the center of the trapdoor and decrease by improving the upper part of the trapdoor. The surface settlement occurring in Case 2 is larger than that occurring in Case 4. The difference between Cases 2 and 4 is the depth of the improved ground, as shown in Table 2. Consequently, based on the test cases with an overburden ratio of 1.0, it is hypothesized that the effect of the ground improvement method increases when the improved depth becomes deeper.

Fig. 6b shows the changes in the maximum surface settlement measured on the profiling line, Line 5, which is located at the center of Trapdoor 2. The horizontal axis represents the displacement from the profiling line to the

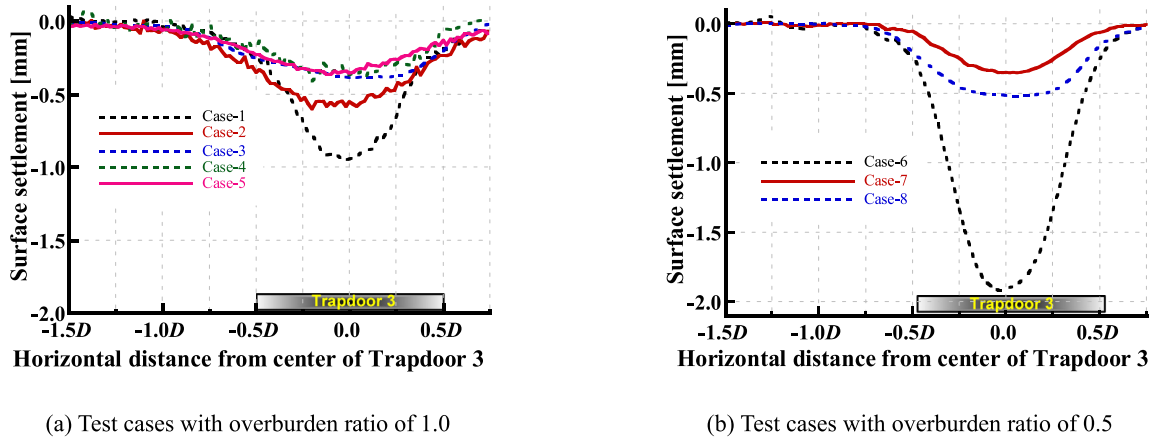


Fig. 5. Surface settlement on Line-8.

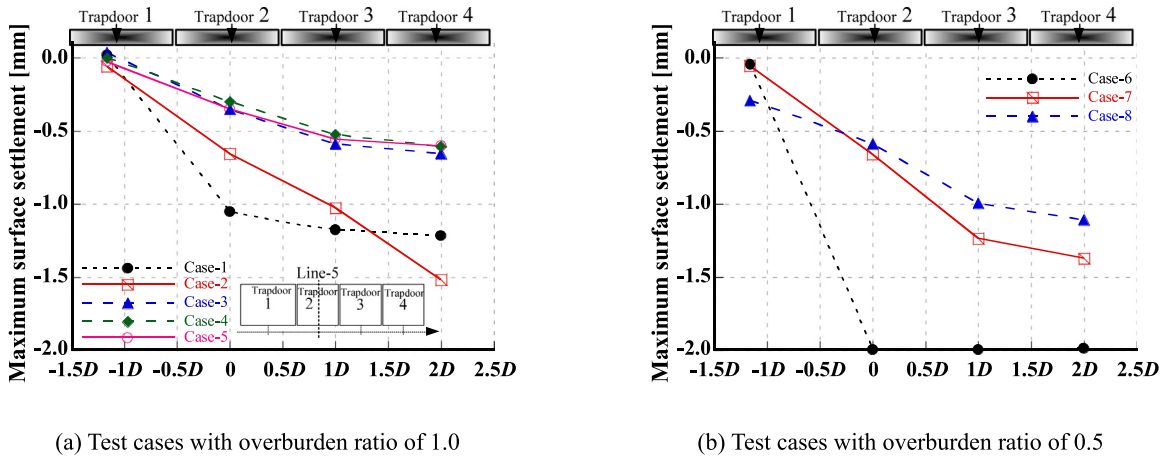


Fig. 6. Maximum surface settlement on Line-5.

tunnel face. The surface settlements are controlled in all of the improved cases. Cases 2 and 4 are different in terms of the height of the improved area, and the surface settlement is attenuated when the height of the improved area is increased. Cases 3, 4, and 5 are different in terms of the width of the improved area; however, the experimental results indicate that the width has almost no effect on the surface settlement.

Surface settlement at H/D of 0.5

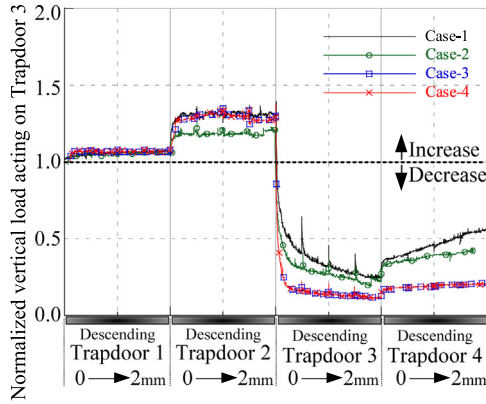
Fig. 5b shows the surface settlement measured on the centerline of Trapdoor 3 (Line 8) after Trapdoor 3 has been lowered to 2.0 mm, for the cases in which the tunnel has been excavated under an overburden ratio of $H/D = 0.5$. The surface settlement in Case 6 shows that the maximum data for the surface settlement are almost the same as the descending displacement of the trapdoor. When the ground has been improved, the surface settlement decreases. When the width of the improved area increases, the effect of the settlement prevention also increases.

Fig. 6b shows the changes in the maximum surface settlement measured on the profiling line, Line 5. The hori-

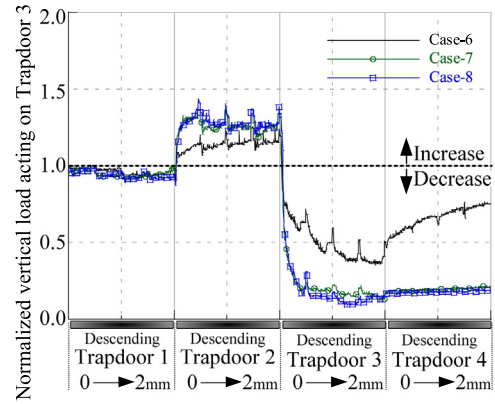
zontal axis represents the displacement from the profiling line to the tunnel face. Almost no preceding settlement (the surface settlement measured on Line 5 when Trapdoor 1 is lowered) occurs in any of the cases. For Case 6, without ground improvement, all of the settlement occurs when the tunnel face arrives at Line 5 (the experimental process that lowers Trapdoor 2), and there is no change in surface settlement when Trapdoors 3 and 4 are lowered. In contrast, in cases in which the ground has been improved, the ground surface continually sinks when Trapdoors 3 and 4 are lowered. Moreover, surface settlement is prevented by the ground improvement, and this effect becomes more prominent as the width of the improved area is increased. This tendency differs, depending on the influence of the width, in cases in which the height of the overburden is 150 mm ($H/D = 1.0$).

Vertical load and earth pressure at H/D of 1.0

Fig. 7a shows the vertical load acting on Trapdoor 3 measured by the load cell that is installed on the underside of the trapdoor plate. In this figure, the vertical load is normalized by the initial vertical load that is measured before



(a) Test cases with overburden ratio of 1.0

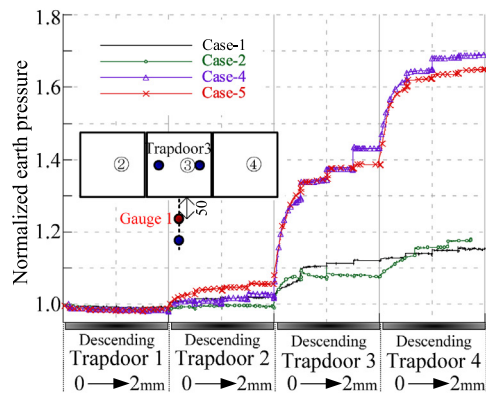


(b) Test cases with overburden ratio of 0.5

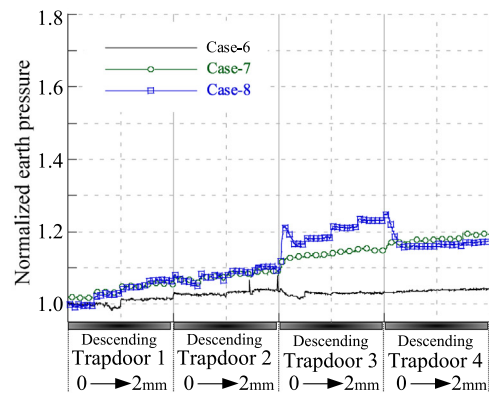
Fig. 7. Normalized vertical load distributions acting on Trapdoor 3 during descending process.

the trapdoors were lowered. No clear change can be found for any of the cases in which Trapdoor 1 is lowered, but the vertical load increases when Trapdoor 2 is lowered. Moreover, the values decrease when Trapdoor 3 is lowered, and they increase again when Trapdoor 4 is lowered. When the ground has been improved, the variations in vertical load are larger than Case 1, which lacks any ground improvement. Comparing Cases 2 and 4, with a difference in height of the improved ground area, the variation in vertical load is large in Case 4, and the height of the improved ground is higher than in Case 2. In contrast, there is almost no difference between Cases 3 and 4 regarding the difference in the width of the improved ground.

Fig. 8a shows the changes in earth pressure that act around Trapdoor 3. The earth pressure increases rapidly when Trapdoors 3 and 4 are lowered. The variations in earth pressure show almost the same values in Cases 1 and 2, and the variations become larger when the height of the improved ground is increased (Case 4). Furthermore, the width of the improved ground has almost no influence on the variation in earth pressure.



(a) Test cases with overburden ratio of 1.0



(b) Test cases with overburden ratio of 0.5

Fig. 8. Normalized earth pressure distributions of Gauge 1 during descending process.

Vertical load and earth pressure at H/D of 0.5

Fig. 7b shows the variation in vertical load acting on Trapdoor 3 for the cases in which the overburdens are 75 mm in height ($H/D = 0.5$). In Fig. 7b, the vertical load is also normalized by the initial vertical load measured before the trapdoors are lowered. For all of the cases, the variations in the normalized vertical load show the same tendency as Cases 1–4 in Fig. 7a. That is, there is almost no change when Trapdoor 1 is lowered, and the vertical load increases when Trapdoor 2 is lowered. Moreover, the normalized vertical load decreases when Trapdoor 3 is lowered, and it increases when Trapdoor 4 is lowered. Despite the fact that the width of the improved areas is different for Cases 7 and 8, the variations in vertical load show almost the same values.

Fig. 8b shows the temporal changes in earth pressure for the cases in which the height of the overburden is 75 mm ($H/D = 0.5$). The earth pressure acting around Trapdoor 3 increases lineally with the progress of the tunnel face in all of the cases. When the upper part of the trapdoor is improved, the variation in earth pressure becomes larger

than that of Case 6. Moreover, the width of the improved ground has almost no influence on the earth pressure.

Discussion on re-distribution of earth pressure

Murayama and Matsuoka (1971) classified three zones through trapdoor experiments, and Costa, Zornberg, Bueno, and Costa (2009) discussed the typical failure mechanisms of trapdoor experiments. In the trapdoor experiments, it is hypothesized that a failure surface initiates at the corners of the trapdoor and propagates toward the center above the trapdoor, as shown in Fig. 9. Zone I, which is surrounded by the failure surface, is deformed identically to the trapdoor vertical displacement. Zone I constitutes a loosened area during the tunnel excavation. Zone II, in Fig. 9, is located at the upper side of Zone I and is also deformed along with the deformation of Zone I. Therefore, the settlement of the ground surface is strongly affected by the deformation of Zones I and II. In contrast, Zone III, in Fig. 9, is located outside of the slip lines and is a steady state area in terms of tunnel excavation.

Based on the concept of Murayama and Matsuoka (1971), the trapdoor experiments in this research work are discussed. Fig. 9 shows the deformation and the re-distribution of the earth pressure obtained from the trapdoor experiments; the location of the improved ground is indicated. In Case 2, the effect of the improved ground is smaller than that in Cases 3 and 4. In this case, the improved ground is located between the slip lines and does not appear in Zone III, as shown in Fig. 9a. Since the improved ground appears in Zone III in other cases, the vertical load of the failure zone can be suitably distributed in Zone III, and surface settlement can thus be prevented.

In the case of a shallow overburden, $H/D = 0.5$, the slip lines develop almost vertically to the surface from the edge of the trapdoor. The distance between two slip lines is almost the same as the width of the trapdoor. When the height of the overburden is increased, the distance between

the slip lines becomes small. When the improved ground is sufficiently wide to intersect the slip lines, the improved ground disrupts the large stress and prevents surface settlement. This effect is increased when the improved area becomes wider but eventually saturates at a certain width of improved area. It is hypothesized that the entire width of the improved ground in Cases 2–5 is larger than this threshold. As a result, the width in these scenarios has no influence on the surface settlement.

The experimental results indicate that when the ground has been improved, the ground surface continually sinks after the cutting face has gone through the measurement line. The influence of the improved ground in the excavation direction is shown in Fig. 10. The improved ground acts as a beam, enlarging the influenced area to an extensive area. As a result, the ground surface sinks continually when the trapdoor is lowered at a location distant from the measurement line.

Numerical analyses

Modeling of ground, lining and tunnel excavation process

To clarify the effect of the ground improvement method, 2D elasto-plastic finite element analyses are conducted. Fig. 11 shows an objective area and boundary conditions. The overburdens in practical construction works, between 2.0 m and 5.25 m ($0.5D$, where D is the tunnel diameter), are applied to the ground improvement method. Therefore, the analyses are performed in the case of an overburden of $D = 0.5$.

The subloading t_{ij} model (Nakai & Hinokio, 2004) is used to simulate the ground material. This constitutive model can properly describe the influence of the intermediate principal stress and the dependence of the direction of plastic flow on the stress paths, density and the confining pressure on the deformation and strength of soils in the t_{ij} -space. The parameters used in this model include the

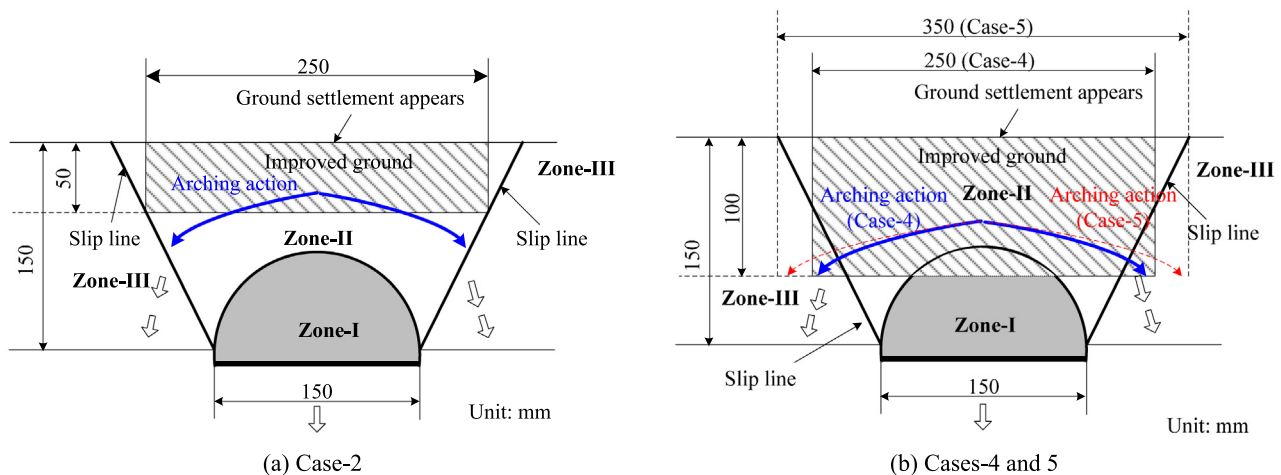


Fig. 9. Deformation and re-distribution of earth pressure with descending trapdoor.

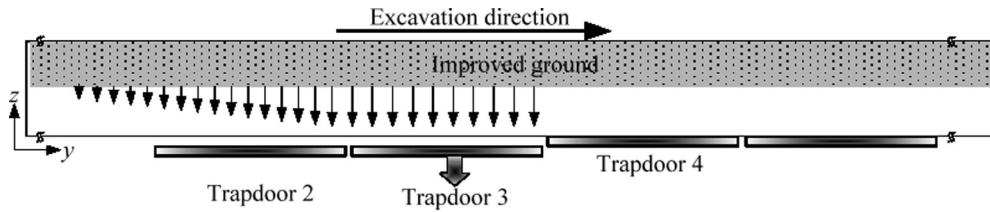


Fig. 10. Influence of improved ground in excavation direction.

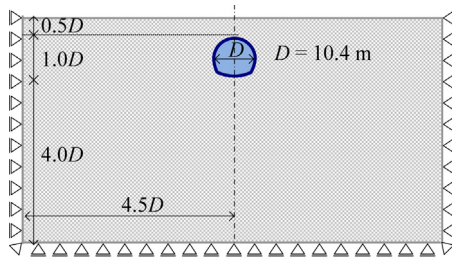


Fig. 11. Objective area and boundary conditions of numerical analyses.

unit weight, γ ; void ratio e ; Poisson’s ratio ν ; principal stress ratio at critical state M_f ; parameter for shape of yield surface, β ; parameter for influence of density and confining pressure, a ; compression index, λ ; and swelling index, κ . The properties of the model ground are given in Table 3. The density ρ and void ratio e are measured by *in situ* tests, while the other parameters are adopted from certain references (Iizuka & Ohta, 1987; Nakai & Hinokio, 2004). The improved ground is modeled as an elastic material. Young’s modulus is calculated based on the compressive strength, q_u ($N = 8 \cdot q_u / 100$, $E = 2800N$). The values used in this analysis are $2.24 \times 10^5 \text{ kN/m}^2$ ($q_u = 1.0 \times 10^3 \text{ kN/m}^2$).

The tunnel lining is modeled as a composite elastic beam unifying the tunnel supports and the shotcrete. First, the parameter of lining, EI , and the parameter of shotcrete, EA , are estimated. The sum of the estimated EI and EA is calculated, and then the parameter of the composite beam is taken to correspond to the summed value. The Young’s modulus of the composite beam is taken as $1.23 \times 10^7 \text{ kN/m}^2$ (Cui, Kishida, & Kimura, 2010).

The tunnel excavating process is simulated by the release of a force equivalent to the excavation. The analysis included seven steps, as shown in Table 4.

Table 3
Input properties of natural ground through numerical works.

| | |
|---|--------|
| Density ρ ($\times 10^3 \text{ kg/m}^3$) | 1.50 |
| Poisson’s ratio ν | 0.36 |
| Void ratio (e_0) | 1.27 |
| Coefficient of earth pressure at rest k_0 | 0.56 |
| Principal stress ratio at critical state | 2.60 |
| Compression index λ | 0.1154 |
| Swelling index κ | 0.02 |

Analytical patterns

Fig. 12 shows the analytical patterns for different widths of the improved areas. The ground is improved around the crown of the tunnel and the top section in Case_a_B. Case_b_B corresponds to the ground that is improved around all of the cross-sections of the tunnel. B, the last part of the case identification, presents the width of each improved area, which varies from 6.0 m to 12.0 m. Only the area around the crown of the tunnel is improved in Case_c.

The improved area of Case_a_7.0 is adopted at an actual construction site, Ushikagi Tunnel (Tohoku Bullet Train line (Hachinohe – Shin Aomori)), that of Case_b_6.5 is adopted for the Kamikita and Akabira Tunnels (Tohoku Bullet Train line (Hachinohe – Shin Aomori)), and that of Case_c is adopted for the Dainiuozu and Uozukaminakajima Tunnels (Hokuriku Bullet Train line (Nagano – Kanazawa)). These three cases represent the basic patterns when determining the areas for the pre-ground improved method.

The aim of the numerical simulation is to elucidate the mechanical behaviors of the ground and the tunnel for the above three cases and the influence of the width and the height of the improved areas.


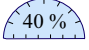




Numerical results and discussion of effect of pre-ground improvement method

Mechanical behavior of original ground

Fig. 13 shows the temporal changes in the settlements of the ground surface, the crown and the foot of the tunnel. Case_0 is the analysis pattern for the excavated tunnel without ground improvement. The ground surface and the tunnel sink with large values in Case_0. Particularly after excavating the bottom section, each settlement in Case_0 rapidly increases, and it is hypothesized that a tunnel collapse occurs during the excavation process. In contrast, the ground surface and the tunnel sink decrease with the improvement of the ground, and the effect is seen to increase in the order of the improved areas (Case_b_6.5 > Case_a_7.0 > Case_c). The percentages in Fig. 13 are the reduction ratios for each settlement value from Case_0.

Fig. 14 shows the surface settlement curves after the tunnel excavations have been completed. The figure indicates that surface settlements can be prevented by adopting the

Table 4
Numerical process of excavation

| Stage No. | Tunnel excavation process | Image |
|-----------|--|---|
| 1 | Initial conditions (initial stress state) | |
| 2 | Equivalent <i>in situ</i> stress of top heading |  |
| 3 | Before installing supports and shotcrete in top heading |  |
| 4 | Support & shotcrete |  |
| 5 | Top heading excavation complete | |
| 6 | Equivalent <i>in situ</i> stress of bottom section |  |
| 7 | Before installing supports and shotcrete in bottom section |  |
| | Support & shotcrete | |
| | Tunnel excavation complete |  |

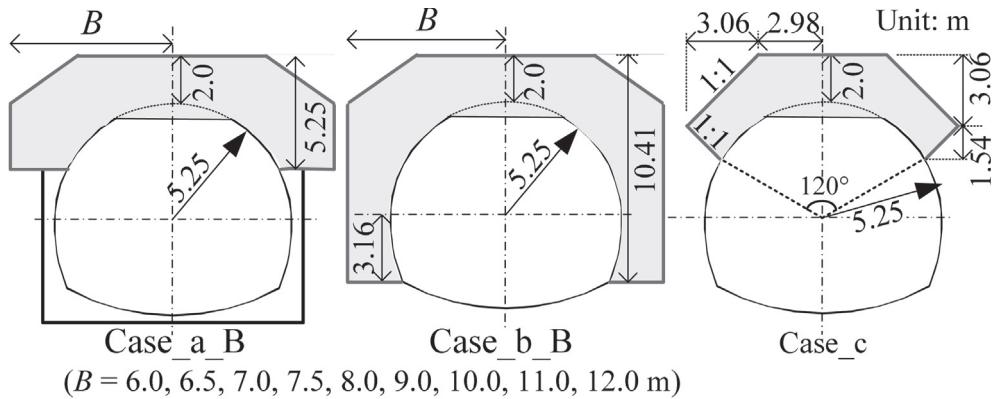


Fig. 12. Analytical patterns for different improved areas.

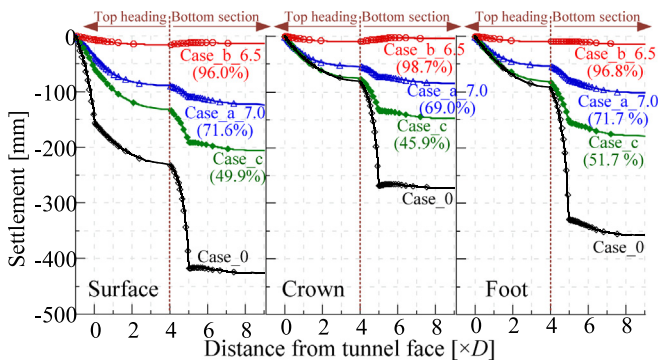


Fig. 13. Temporal changes in settlements of ground and tunnel and reduction ratio for each settlement from Case₀.

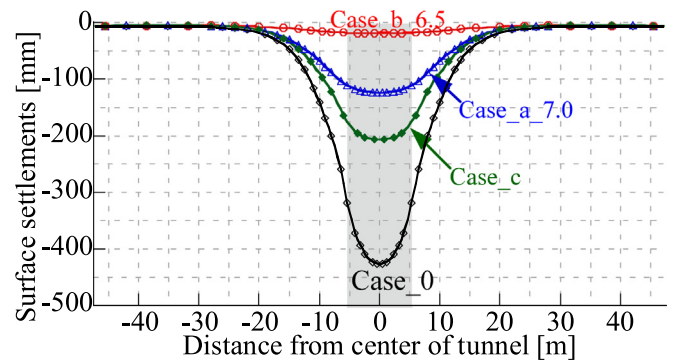


Fig. 14. Ground surface settlements at completion of tunnel excavation.

pre-ground improvement method and that the method becomes more effective as the improved area becomes larger. The horizontal displacements occurring in the marked ground areas (Lines 1, 2 and 3), when the tunnel excavations have been completed, are shown in Fig. 15. The dis-

tance between the center of the tunnel lining and Lines 1–3 is 7.5 m, 10.0 m and 15.0 m, respectively. The ground is displaced toward the tunnel lining due to the tunnel excavation, and the largest horizontal displacements occur on the ground surface in all of the cases and examination positions. The horizontal displacements decrease as the areas of

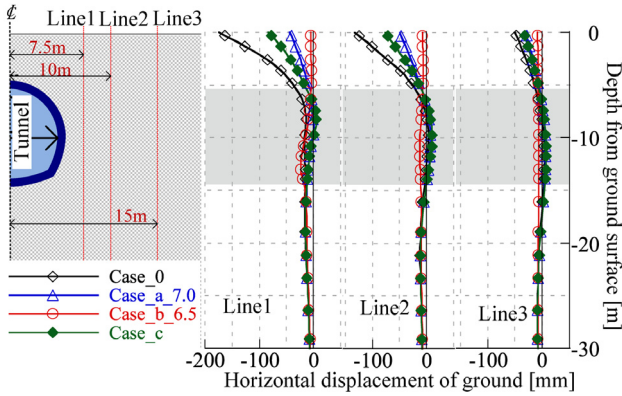


Fig. 15. Horizontal displacement distributions at completion of tunnel excavation.

the improved ground increase. In particular, almost no displacement can be detected in Case_b_6.5, for which all cross-sections of the tunnel are improved.

Fig. 16 shows the vertical earth pressure distribution on two kinds of horizontal lines, namely, the spring line and the tunnel foot, after the tunnel excavations have been completed. The straight dotted lines show the initial vertical earth pressure distribution. The full black lines without markers, show the vertical earth pressure distribution for Case_0, in which the tunnel is excavated without ground improvement. The figure shows that the vertical earth pressure, which acts on both sides of the tunnel, increases in a certain area due to the tunnel excavation. The vertical earth pressure acting on Lines I and II is concentrated in the improved area, and the influenced area becomes narrow in Case_b_6.5. This effect is called the earth pressure redistribution effect. However, there is almost no change in the influenced area for either Case_a_7.0 or Case_c.

The shear strain distributions for the two analysis stages, namely, when the top heading has been excavated and when all cross-sections of the tunnel have been excavated, are shown in Fig. 17. In Case_0, for a tunnel excavated in a natural ground, large shear strain is generated

at the foot of the tunnel, and a zone of shear strain appears from the tunnel spring line to the ground surface. When ground improvement has been conducted, the shear strain zone from the tunnel spring line to the ground surface is intercepted by the improved area. As a result, the shear strain decreases due to the improved ground; this effect is called the shear reinforcement effect. However, for Case_a_7.0 and Case_c, the improved area is not sufficiently wide to intercept all of the large shear strain area. As a result, large shear strain remains around the improved area, although this strain is attenuated when the improved area becomes wider. When all the cross-sections of the tunnel have been improved, as in Case_b_6.5, the improved ground can intercept the large shear strain, despite the width of the improved ground.

Mechanical behavior of improved ground

Fig. 18 shows the deformation of the improved ground. To facilitate understanding, the deformation is magnified by a factor of 50. The dotted lines represent the original position of the improved ground. The deformation of the improved ground decreases when the improved areas become larger. The deformation of the improved ground shows the same shapes in Case_a_7.0 and Case_c; the upper part of the improved ground is compressed, and both ends of the improved ground move away from the tunnel. In contrast, both ends of the improved ground move towards the center of the tunnel in Case_b_6.5. This deformation shape is the same as the deformation of the tunnel lining, indicating that the improved ground can suppress the deformation of the tunnel lining.

Influence of width and height of improved area

The reduced ratios of the settlements of the ground surface and the tunnel for different widths of the improved area are shown in Fig. 19. The analytical results indicate that the settlement-preventing effect increases when the width of the improved area becomes larger. For Case_a_B, the reduced ratios of the settlements increase rapidly when

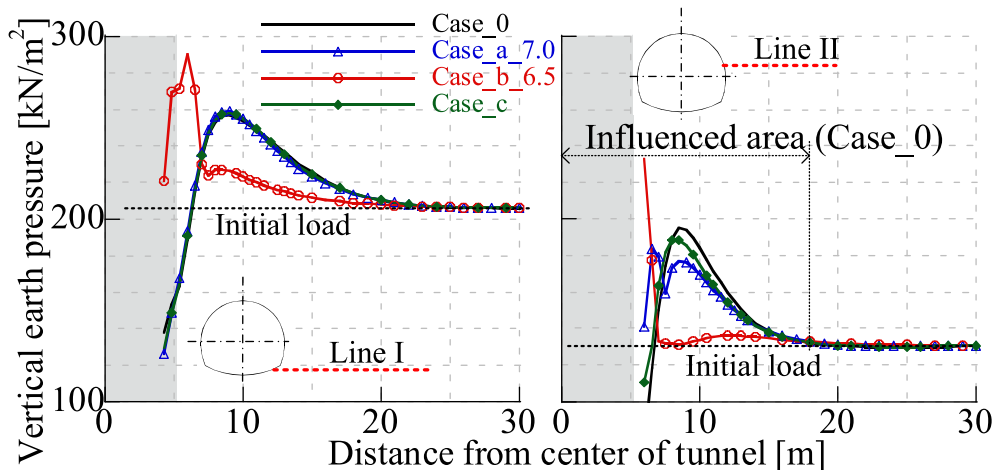


Fig. 16. Vertical earth pressure distributions on two horizontal lines.

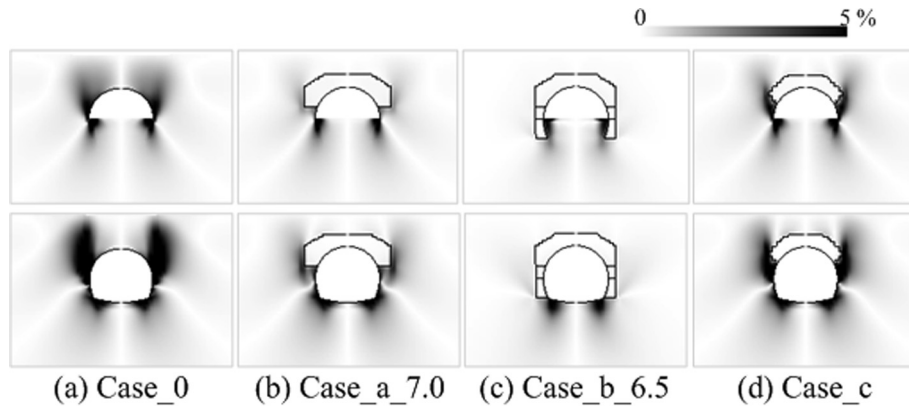


Fig. 17. Shear strain distributions through numerical works.

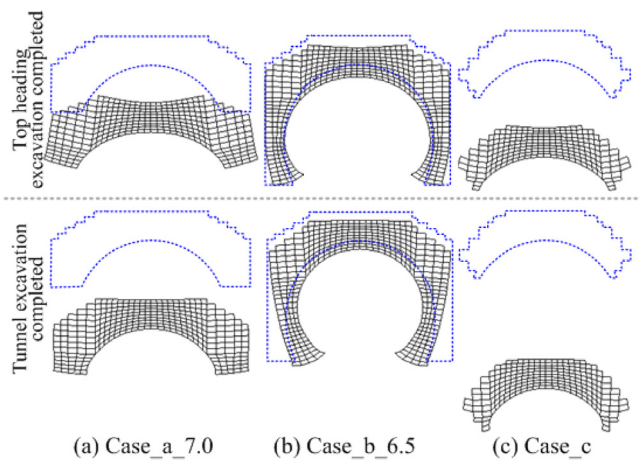


Fig. 18. Deformation of improved ground through numerical works.

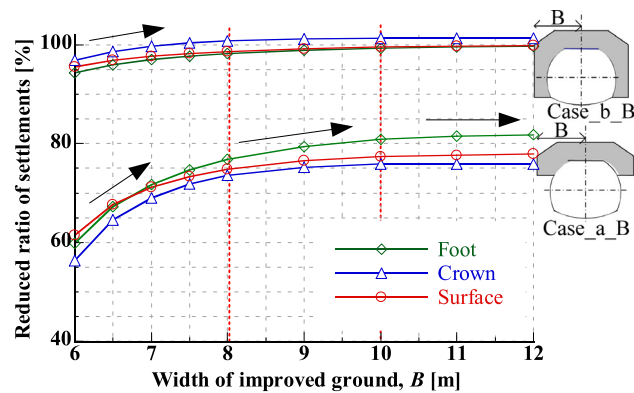


Fig. 19. Reduction ratios of settlement are plotted along width of improved ground, B.

the widths are smaller than 8 m; they reach a peak of 90% when the widths are larger than 10.5 m. For Case_b_Bs, the reduced ratio of the settlements of the tunnel and the ground is larger than 95% in all of the cases.

A series of numerical analyses that varied the height of the improved area is performed in this research work. Fig. 20 shows the reduced ratios of the settlements of the ground surface and the tunnel for different heights of the improved area. The analytical results indicate that the

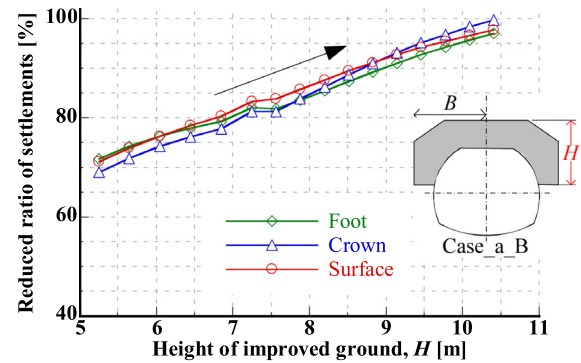


Fig. 20. Reduction ratios of settlement are plotted along height of improved ground, H.

settlement-preventing effect increases when the height of the improved area becomes larger and that the relationship is linear.

Design concept of improved ground tunnel excavation

Through the 3D trapdoor experiments and the numerical simulations, the effect of the improvement tunneling method is confirmed by the prevention of the deformation on the tunnel excavation process and the stability of the tunnel face. The shape of the improved area, the stability of the tunnel cross-sections, and the longitudinal section of the tunnel are all discussed in this section. In addition, the design concept for improved ground tunnel excavation is presented.

Shape of improved area

The slip lines and the improved area are described in Fig. 21. A slip line is a zone where the shear strain is concentrated and easily detectable; it is the identical the shear zone in the numerical simulation of a tunnel excavation. In the case of a top-spring line improvement, the slip line is confined by the improved ground. Consequently, it can be clearly confirmed that settlement on the tunnel excavation is prevented. When the bottom heading is excavated, the improved area deforms in the vertical direction. In this

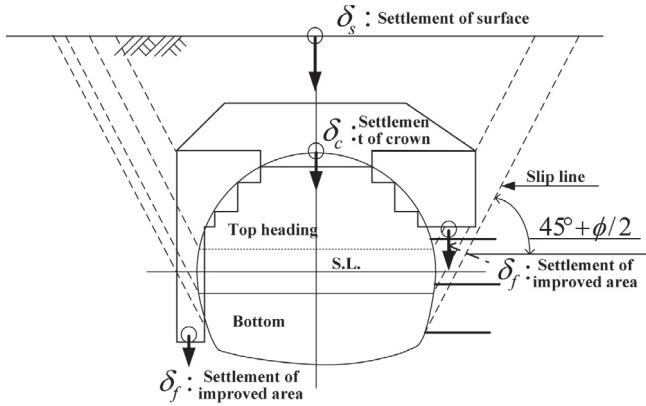


Fig. 21. Slip lines which appear in each excavation stage and location of improved area.

case, therefore, the prevention of settlement cannot clearly be confirmed. In the case of a gate-type improved area, however, the slip line is confined by the improved area on both the top heading and the bottom heading excavations. The bottom edge of the improved area is located at Zone III in Fig. 9. The prevention of settlement is clearly effective.

It is hypothesized that an improved area must be installed at the loosened zone of cross-sections. The areas of Zones I and II in Fig. 9 are decreased since an improved area has been installed; the improved area must re-distribute the load of the loosened zone to Zone III.

Stability of tunnel cross-sections

Since the slip line at the tunnel excavation is confined by the improved ground, settlement can be prevented. However, it is confirmed that vertical loads are applied at the bottom of the improved ground. Consequently, re-distribution of an additional vertical load and the associated stress concentration occur at the original ground, which is located at the bottom of the improved ground. Since the improved area exists in the direction of the tunnel excavation, it strongly contributes to the stability of the tunnel face and the stress re-distribution against the excavation. To consider the tunnel stability of cross-sections, the stability of the ground located under the improved area is discussed. Since the improved tunnel method should be conducted at the shallow overburden field, particularly where the overburden is less than D , the equilibrium of only the vertical loads are considered.

Fig. 22 shows the loads at both the top heading excavation and the bottom excavation in the case of the improved area, which is installed in the upper part of the objective tunnel. During the tunnel excavation, the self-weight of the ground located in the upper part of the improved area, αP_v , and that of the improved ground, αW , are applied in the downward direction. In addition, the frictional resistance at the boundary between the side line of the improved area and the original ground is also applied in an upward

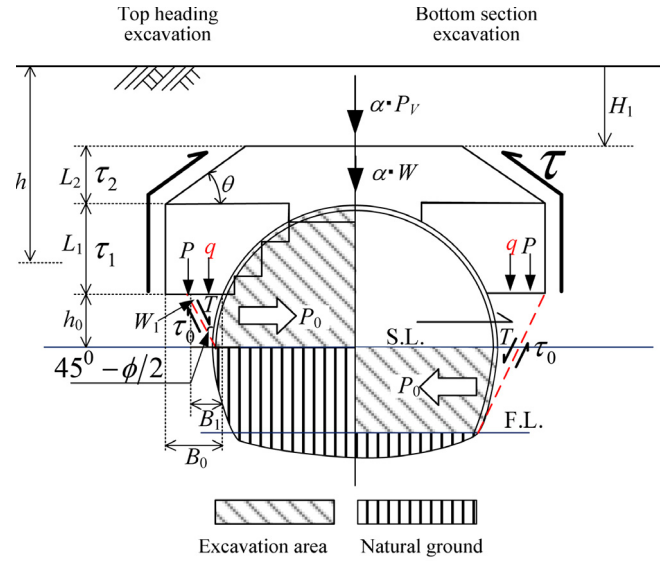


Fig. 22. Relative position between slip line and improved ground in case of improved arch part.

direction. P_v is the vertical earth pressure at the tunnel excavation, W is the lining load from the improved ground, and α is the coefficient of the stress re-distribution. At the side line of the improved ground, in the range of L_1 in Fig. 22, the frictional resistance, τ_1 , is described as follows:

$$\tau_1 = c \cdot L_1 + K_0 \cdot \gamma_t \cdot \tan \phi \cdot L \int_{H_1+L_2}^{H_1+L_2+L_1} h dh, \tag{1}$$

where K_0 is the coefficient of earth pressure at rest, c is cohesion, γ_t is the unit weight, and ϕ is the internal friction angle, respectively. L_1 and L_2 are defined as the length range parameter, which is shown in Fig. 22. In addition, the vertical component of the frictional resistance in an inclined part of the improved ground, τ_2 , is described as follows:

$$\tau_2 = c \cdot L_2 \cdot \sin \theta + K_0 \cdot \gamma_t \tan \phi \cdot L \cdot \sin \theta \int_{H_1}^{H_1+L_2} h dh. \tag{2}$$

From Eqs. (1) and (2), the vertical component of the frictional resistance force on the improved ground, τ , is $\tau = \tau_1 + \tau_2$. Therefore, the vertical force, P , which is applied on the bottom line of the improved ground, is described as follows:

$$P = (\alpha P_v + \alpha W - \tau) / 2. \tag{3}$$

P acts on the original ground on the bottom line of the improved ground whose length is B_0 , as shown in Fig. 22. Comparing P with the allowable bearing capacity of the original ground, the stability of the tunnel excavation can be discussed.

As for the top heading excavation, a movable soil mass, such as weight W_i , shown in Fig. 22, appears. When the bottom part is excavated, the slip line runs from the foot line of the tunnel to the corner of the improved ground, as shown in Fig. 22. The movable soil mass becomes larger

than that at the top heading excavation. The shear stress along the slip line is expressed in Eq. (4) by considering the weight of the movable soil mass, W_i ; the vertical load from the improved ground to the movable soil mass, q ; the height of the movable soil mass, h_0 ; and the angle of the slip line, θ_0 .

$$\tau_0 = \{(W_i + q) \sin \theta_0 \cdot \tan \phi + c\} \cdot h / \cos \theta_0. \quad (4)$$

The slip force at the movable soil mass, T , is expressed as follows:

$$T = (W_i + q) \cos \theta_0. \quad (5)$$

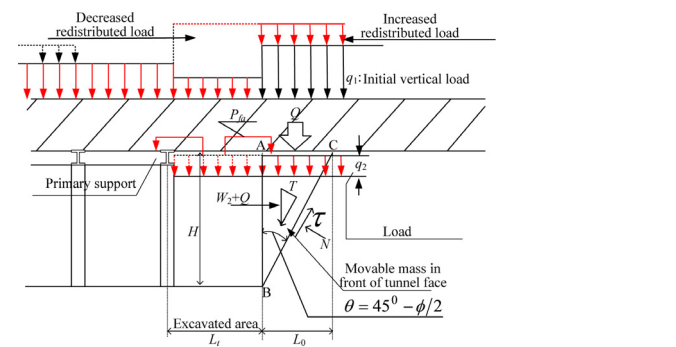
Therefore, the safety factor of the movable soil mass, R_s , is defined as follows:

$$R_s = \tau_0 / T. \quad (6)$$

When installing the improved ground in the range of the upper area, as shown in Fig. 22, the confining effect of the slip line at the bottom excavation is small. When installing the improved ground in the range from top to bottom, the slip line at the bottom excavation includes the improved ground. Therefore, the improved method has the advantage of a confining effect on the slip line. In this case, it must be confirmed that the allowable bearing capacity of the original ground can accommodate the vertical force acting from the improved ground.

Stability of longitudinal section

Fig. 23 shows the stress re-distribution along the longitudinal section through the field measurements and laboratory experiments. In the longitudinal section, the improved ground behaves as a beam. During an excavation, the vertical load at the tunnel crown is distributed in front of the tunnel excavation face. However, the acting vertical load on a movable mass, triangle ABC in Fig. 23, does not



- q_1 : Initial vertical load L_i : Spacing of steel lining
 W_2 : Mass weight of movable area in the front of tunnel face
 c : Cohesion H : Height of tunnel face
 ϕ : Internal friction angle
 Q : Applied load on movable area in front of tunnel face,
 T : Sliding force along line-BC, $(W_2 + Q)\cos\theta$,
 τ : Frictional resistance force along line-BC, $(W_2 + Q)\cos\theta \cdot \tan\theta + cH/\cos\theta$,
 N : Normal force along line-BC, P_{σ} : Re-distributed applied force due to tunnel excavation

Fig. 23. Load distribution at tunnel crown in longitudinal direction when top heading is excavated.

increase, since the improved ground produces a load on the beam. The vertical load in the range of the tunnel excavation decreases relative to the case of no installed improved ground. The stability of the tunnel excavation face is considered in terms of the slip force along BC-line in Fig. 23, T , and the shear resistance force, τ_0 . The safety factor, R_{sl} , is defined as

$$R_{sl} = \tau_0 / T. \quad (7)$$

Based on the field measurements and the laboratory experiments, it is hypothesized that the vertical load acting on the movable mass is decreased. In contrast, the shear resistance force is increased since the cohesion and the internal friction angle are increased by installing improved ground. In addition, the improved ground is located in both side areas. This configuration provides an advantage in terms of the stability of the tunnel face. Consequently, the safety factor, R_{sl} , increases with the installation of the improved ground.

Conclusions

Through trapdoor experiments and numerical simulations, the stability of a shallow overburden tunnel and the mechanism of a ground improvement method were evaluated. In addition, a design method was discussed.

A series of experiments that varied the height of the overburden and the size of the improved area was performed in this study, and the experimental results indicate that the pre-ground improvement method can prevent ground settlement and can increase the stabilization of the cutting face of tunnels. In the cross-section of the tunnel, the relative position between the slip line and the improved ground is hypothesized to be the major cause of the different tendencies in the influence of the width of the improved ground under these two different overburden conditions. The slip lines occurring due to the lowering of the trapdoor under different conditions are shown in Fig. 9. In an actual tunnel excavation, the relative relation between the slip line and the improved ground is considered in Figs. 21 and 22. When the improved ground is sufficiently wide to intersect the slip lines, the improved ground disrupts the large stress and prevents surface settlement. This effect increases as the improved area becomes wider; however, there is a limited width above which the effect does not change.

The experimental results indicate that when the ground has been improved, the ground surface continually sinks after the cutting face has passed through the measurement line. The influence of the improved ground in the excavation direction is shown in Fig. 23. From the experimental results in Fig. 8, the vertical load on excavated area is applied to the surrounding ground. Therefore, the vertical load ahead of the excavated direction is increased. The improved ground acts as a beam, enlarging the influenced area extensively. As a result, the ground surface sinks con-

tinually when the trapdoor is lowered at a location distant from the measurement line.

Through the numerical work, the effect of the pre-ground improvement method and the influence of the width and height of the improved area were confirmed. Thus, the ground improvement method can prevent settlement of the ground and the tunnel, and this effect becomes more effective as the width and the height of the improved area increases. The influenced area due to the tunnel excavation becomes narrow when the ground surrounding the cross-sections of the tunnel lining is improved. The height of the improved ground has a larger influence than the width of the improved ground on the prevention of settlements. Therefore, the advantage of the ground improved method is presented as three issues, namely, the effect of shear reinforcement, the effect of earth pressure redistribution and the effect of ground reinforcement. These three effects become even more effective as the width and the height of the improved ground increase.

References

- Adachi, T., Kimura, M., & Kishida, K. (2003). Experimental study on the distribution of earth pressure and surface settlement through three-dimensional trapdoor tests. *Tunnelling and Underground Space Technology*, 18(2–3), 171–183. [http://dx.doi.org/10.1016/S0886-7798\(03\)00025-7](http://dx.doi.org/10.1016/S0886-7798(03)00025-7).
- Costa, Y., Zornberg, J., Bueno, B., & Costa, C. (2009). Failure mechanisms in sand over a deep active trapdoor. *Journal of Geotechnical and Geoenvironmental Engineering, ASCE*, 135(11), 1741–1753. [http://dx.doi.org/10.1061/\(ASCE\)GT.1943-5606.0000134](http://dx.doi.org/10.1061/(ASCE)GT.1943-5606.0000134).
- Cui, Y., Kishida, K., & Kimura, M., 2010. Analytical study on the control of ground subsidence arising from the phenomenon of accompanied settlement using footing reinforcement pile. Deep and Underground Excavation, ASCE Geotechnical Special Publication, pp. 307–312, DOI: 10.1061/411107(380)42.
- Cui, Y., Kishida, K., & Kimura, M. (2008). Experimental study on effect of auxiliary methods for simultaneous settlement at subsurface and surface during shallow overburden tunnel excavation. *Japanese Geotechnical Journal*, 3(3), 261–272. <http://dx.doi.org/10.3208/jgs.3.261>.
- Iizuka, A., & Ohta, H. (1987). A determination procedure of input parameters in elasto-viscoplastic finite element analysis. *Soils and Foundations*, 27(3), 71–87.
- Kamata, H., & Mashimo, H. (2003). Centrifuge model test of tunnel face reinforcement by bolting. *Tunnelling and Underground Space Technology*, 18(2–3), 205–212. [http://dx.doi.org/10.1016/S0886-7798\(03\)00029-4](http://dx.doi.org/10.1016/S0886-7798(03)00029-4).
- Kimura, H., Ito, T., Iwata, M., & Fujimoto, K. (2005). Application of new urban tunneling method in Baikoh tunnel excavation. *Tunnelling and Underground Space Technology*, 20(2), 151–158. <http://dx.doi.org/10.1016/j.tust.2003.11.007>.
- Kitagawa, T., Goto, M., Tamura, T., Kimura, M., Kishida, K., Cui, Y., & Yashiro, K. (2009). Experimental studies on tunnel settlement reduction effect of side piles. *Doboku Gakkai Ronbunshuu F, JSCE*, 65(1), 73–83. <http://dx.doi.org/10.2208/jscejf.65.73>.
- Kitagawa, T., Goto, M., Tamura, T., Kimura, M., Kishida, K., Yashiro, K., & Shimamoto, K. (2010). Numerical analyses of tunnel settlement reduction effect by side piles. *Doboku Gakkai Ronbunshuu F, JSCE*, 66(1), 85–100. <http://dx.doi.org/10.2208/jscejf.66.85>.
- Kitagawa, T., Isogai, A., Okutsu, K., & Kawaguchi, T. (2004). Excavation through Earth Ground with Small Burden by Soil Improvement and Side Pile – Ushikagi Tunnel on Tohoku Shinkansen Line. *Tunnels and Underground, JTA*, 35(4), 255–262 (in Japanese).
- Miwa, M., & Ogasawara, M. (2005). Tunnelling through an embankment using all ground fasten method. *Tunnelling and Underground Space Technology*, 20(2), 121–127. <http://dx.doi.org/10.1016/j.tust.2003.12.001>.
- Murayama, S., & Matsuoka, H. (1971). Earth pressure on tunnels in sandy ground. *Proceedings of JSCE*, 187, 95–108 (in Japanese).
- Nakai, T., & Hinokio, M. (2004). A simple elastoplastic model for normally and over consolidated soils with unified material parameters. *Soils and Foundations*, 44(2), 53–70.
- Nakai, T., Xu, L. M., & Yamazaki, H. (1997). 3D and 2D model tests and numerical analyses of settlements and earth pressures due to tunnel excavation. *Soils and Foundations*, 37(3), 31–42.
- Nonomura, M., Iura, T., Okajima, M., & Kishida, K. (2011). Effectiveness and issues of pre-improvement of unconsolidated ground for shall tunnel construction. *Tunnels and Underground, JTA*, 42(5), 381–391 (in Japanese).
- Oke, J., Valchopoulos, N., & Marinos, V. (2014). Umbrella arch nomenclature and selection methodology for temporary support systems for the design and construction of tunnels. *Geotechnical and Geological Engineering*, 32(1), 97–130. <http://dx.doi.org/10.1007/s10706-013-9697-4>.
- Ono, R., & Manai, K. (1938). Vertical earth pressure on dry sand layer. *Civil Engineering, JSCE*, 24(5), 437–459 (in Japanese).
- Saito, S., Ishiyama, T., Tano, S., & Haga, H. (2011). Behaviour of tunnel ground-stabilized to the formation level: Kamikita Tunnel and Akahira Tunnel, Tohoku Shinkansen. *Tunnels and Underground, JTA*, 39(6), 399–406 (in Japanese).
- Tadenuma, Y., Isogai, A., Konishi, S., Nishiyama, T., & Okutsu, K. (2003). Excavation of a shallow tunnel with ground stabilization. *Proceedings of Tunnel Engineering, JSCE*, 13, 207–212 (in Japanese).
- Taguchi, Y., Kagawa, K., Sagara, M., & Oshikawa, K. (2000). Reinforcing effects of thin flexible pre-lining. *Journal of Geotechnical Engineering, JSCE*, 654/III-50, 125–135 (in Japanese).
- Yoo, Chungsik. (2002). Finite-element analysis of tunnel face reinforced by longitudinal pipes. *Computers and Geotechnics*, 29(1), 73–94. [http://dx.doi.org/10.1016/S0266-352X\(01\)00020-9](http://dx.doi.org/10.1016/S0266-352X(01)00020-9).